

# Time-frequency equivalence using chirp signals for frequency response analysis

Resmi Suresh

Indian Institute of Technology Guwahati <https://orcid.org/0000-0002-7401-5390>

Raghunathan Rengaswamy ([✉ raghur@iitm.ac.in](mailto:raghur@iitm.ac.in))

Indian Institute of Technology Madras

---

## Article

**Keywords:** Frequency Response Analysis, Nyquist plot, Impedance, Chirp signals, EIS

**Posted Date:** March 11th, 2021

**DOI:** <https://doi.org/10.21203/rs.3.rs-134038/v1>

**License:**  This work is licensed under a Creative Commons Attribution 4.0 International License.

[Read Full License](#)

---

1 Time-frequency equivalence using chirp signals for frequency  
2 response analysis

3 Resmi Suresh<sup>1,\*</sup> and Raghunathan Rengaswamy<sup>2,\*</sup>

4 <sup>1</sup>Indian Institute of Technology Guwahati, India

5 <sup>2</sup>Indian Institute of Technology Madras, India

6 December 22, 2020

7 **Abstract**

8 Frequency response analysis (FRA) of systems is a well-researched area. For years, FRA has been  
9 performed using input signals, which are a series of sinusoids or a sum of sinusoids. This results in  
10 large experimentation time, particularly when the system has to be probed at lower frequencies. In this  
11 work, we describe a previously unknown time-frequency duality for linear systems when probed through  
12 chirp signals. We show that the entire frequency response can be extracted with a single chirp signal by  
13 extending the notion of instantaneous frequency to both the input and output signals. It is surprising  
14 that this powerful result had not been uncovered given that FRA has been used in multiple disciplines  
15 for more than hundred years. This result has the possibility of completely revolutionizing methods used  
16 for frequency response analysis. Simulation studies that support the main result are described. While  
17 this result is of relevance in multiple areas, we demonstrate the potential impact of this result in electro-  
18 chemical impedance spectroscopy.

19 **Keywords:** Frequency Response Analysis, Nyquist plot, Impedance, Chirp signals, EIS

21 **1 Introduction**

22 A system can be characterized by how it responds to sinusoidal input perturbations, also known as the  
23 frequency response analysis (FRA). The frequency response at a particular frequency can be specified as a  
24 ratio of the output to input, represented as a complex number. Since frequency response is computed from  
25 time series data, an equivalence between time and frequency needs to be established. This is directly realized  
26 through the well-known Fourier Transform, which allows any time domain signal to be decomposed into its  
27 constituent frequency components. A standard approach for FRA of a system is to perturb the system with  
28 an input, which is usually a series of sine signals or a sum of sine (multi-sine) signal [29, 25] and identify  
29 the frequency response from the output data. A key observation here is that to generate one point in the  
30 frequency domain, all the time domain data needs to be processed. This is referred to as the localization  
31 problem. A direct consequence of this problem is that large experimentation times are needed for generating  
32 the complete frequency response of the system and there are also other issues related to deconvolution of  
33 the various frequency components from the time domain signal.

34 There have been several attempts that have been made over the years to address the localization problem  
35 [17, 11]. The ideal case would be for a single time point to be localized to a single frequency, which  
36 is theoretically not possible. Short term Fourier transforms (STFT) [1] and Wavelet transforms (WT)  
37 [11, 17] are some of the time frequency localization approaches that have been attempted. Hilbert-Huang-  
38 Transforms (HHT) is another approach that is focused on addressing this problem [16]. In HHT, from  
39 a time domain signal, the so called intrinsic mode functions (IMF) are extracted, which are as close to  
40 monochromatic as possible. Hilbert transforms of the IMF then provide some measure of time frequency  
41 localization. However, none of these techniques (STFT, WT, HHT) specifically focus on generating an exact  
42 time frequency equivalence.

43 Another approach towards time frequency localization is the use of chirp signals [13, 8, 5, 15]. The interest  
 44 in chirp signals is due to the fact that it is possible to define a "so called" instantaneous frequency, which is a  
 45 differential of the phase function of a sinusoid. As a result, a notional frequency can be assigned to every time  
 46 point in the input signal. Although this notion of one-to-one mapping between time and frequency could  
 47 be carried over to the output response for linear systems, work in extant literature is focused exclusively  
 48 on using chirp signals for data generation to be processed by other techniques such as STFT [10, 30, 26]  
 49 or WT [3] and less on exploring the implications of the interesting time-frequency localization that chirp  
 50 signals afford. This might also be because instantaneous frequency as a concept itself is not well accepted  
 51 and/or understood [4, 21]. There has been interest in interpreting instantaneous frequency and exploring  
 52 connections between standard techniques such as FFT and chirp, but still only in terms of information  
 53 content in the signal and not from viewing two time series (input and output) as having the same frequency  
 54 variation across time [21, 20]. Our prior work [6, 28] comes closest to exploring the time-frequency equivalence  
 55 proposed here; however, we just proposed an algorithm for FRA of electrochemical systems. We claimed  
 56 that our algorithm was an approximate method for FRA; the impact of time-frequency equivalence was  
 57 neither clearly understood nor carefully explored at that time. Summarizing, a fundamental question that  
 58 is of interest is the following: is there a direct one-to-one equivalence between the time domain behavior and  
 59 the frequency domain behavior that can be established by assigning a single frequency to every time point in  
 60 a time series data? In this paper, we describe an unexplored equivalence in the case of linear systems when  
 61 the two time series data (input and output) are hypothesized to possess the same one-to-one time-frequency  
 62 mapping. This equivalence allows the direct computation of the frequency characteristics from time domain  
 63 data without ever performing any transformations. It also substantiates the usefulness of the previously  
 64 hypothesized instantaneous frequency. Finally, the result is an asymptotic result, much in the same format  
 65 as the well-known time frequency equivalence result for a single frequency input perturbation. In this paper,  
 66 we discuss the main result and various computational studies that validate the main result. For the sake of  
 67 brevity, we present the significance of the main result and its implications in this paper. A detailed proof in  
 68 support of the main result and other mathematical details are available in [27].

## 69 1.1 Preliminaries

A chirp signal is a signal with time-varying frequency. The generic form of a chirp signal is  $u(t) = A \sin(\phi(t))$  where  $\phi(t)$  is the instantaneous phase. The instantaneous angular frequency of the signal at any instant  $t$  is defined as the differential of the instantaneous phase of the sinusoid at time  $t$  ( $\omega(t) = 2\pi f(t) = d\phi(t)/dt$ ). One can see from the definition of chirp signal that the phase function  $\phi(t)$  is not assumed to take any particular form. Linear chirp defined below has been a popular choice.

$$\text{Linear Chirp: } u(t) = \sin(\phi_0 + 2\pi(f_0 t + 0.5h_1 t^2)) \quad (1)$$

70 where  $f(t) = f_0 + h_1 t$  is the linear instantaneous frequency and  $\phi_0$  is the initial phase. One could generalize  
 71 this linear chirp to  $n^{th}$  order polynomial chirp, whose phase function  $\phi(t) = P_{n+1}(t)$ , is an  $(n+1)^{th}$  order  
 72 polynomial.

## 73 2 Results

74 We start with a very well-known result in the area of system identification.

**Lemma 1.** *When a stable, strictly causal linear system  $G(s)$  is perturbed with an input sine signal ( $u_s(t) = A_{in} \sin \omega t$ ;  $\omega = 2\pi f$ ), as time  $t$  tends to infinity, output of the system  $x(t)$  is also a sine signal with the same frequency as the input but with an amplitude ratio and phase lag.*

$$x(t) = A_{in} AR(\omega) \sin(\omega t + \phi_L(\omega)) + E(t) \quad (2)$$

where  $AR(\omega)$  and  $\phi_L(\omega)$  are the amplitude ratio and phase lag at angular frequency  $\omega$ . Also,  $E(t) = 0$  and  
 $t \rightarrow \infty$ , thus,

$$x(t) = A_{in} AR(\omega) \sin(\omega t + \phi_L(\omega)) \quad (3)$$

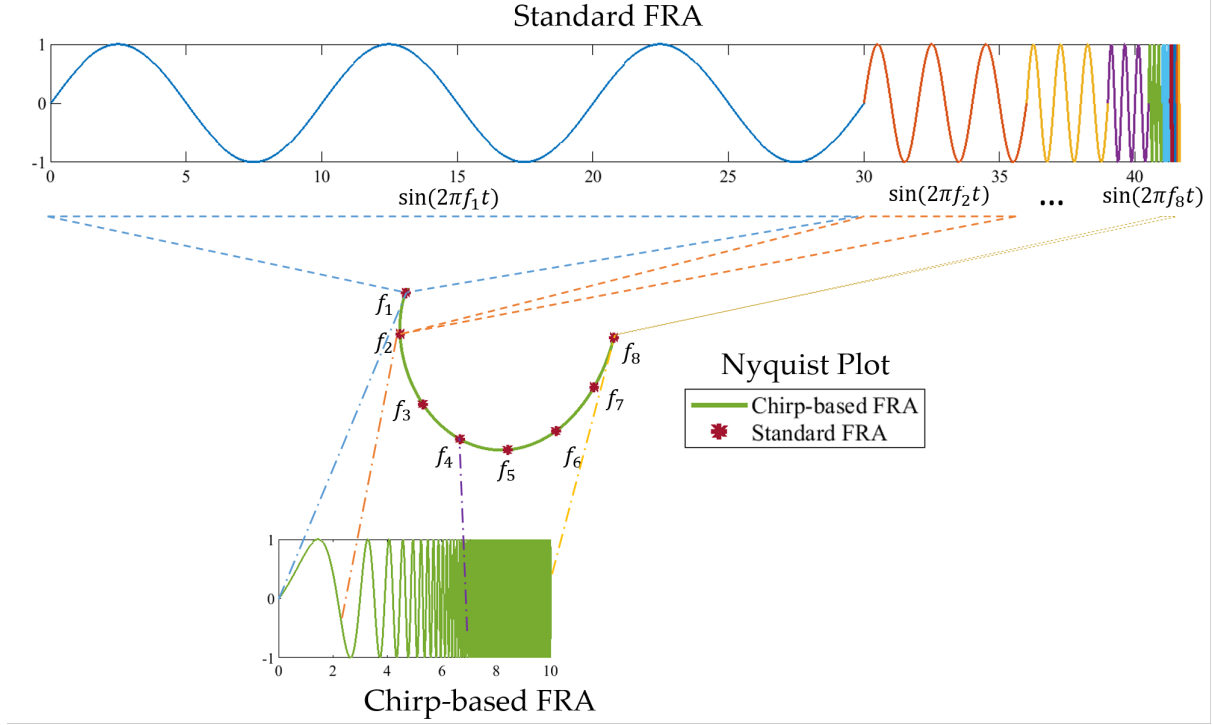


Figure 1: Comparison of the working of standard FRA and chirp-based FRA. Standard FRA uses a few cycles of multiple sinusoidal signals of different frequencies to obtain discrete points in the Nyquist plot. Chirp-based FRA generates as many points in Nyquist plot as the number of samples in the output signal and thus, a smooth and continuous impedance profile is obtained in a short time.

This result has been used for decades now and is the foundation on which FRA has progressed. Using this result, the frequency response of the system as a complex number can be identified at each frequency by perturbing the system at every frequency of interest. However, a major disadvantage of this result is that, to derive the complete frequency response, the system has to be perturbed at several frequencies individually. This is sometimes simplified using a sum of sines input and deconvolution of the output using fast Fourier transform (FFT) [7]. Notice that this is an asymptotic result and hence one would have to wait for a certain amount of time for the transients to dissipate before the frequency response is identified. We now present the main result derived in this paper and contrast that with Lemma 1.

**Main Result.** *When a stable, strictly causal linear system  $G(s)$  is perturbed with a chirp signal ( $u(t) = A_{in} \sin \phi(t)$ ), as time  $t$  tends to infinity, the output of the system is also a chirp signal such that the instantaneous amplitude ratio ( $AR^{ch}$ ) and phase lag ( $\phi_L^{ch}$ ) of the chirp signal are same as the true amplitude ratio and phase lag of the system corresponding to the instantaneous frequency.*

$$x(t) = A_{in} AR^{ch}(t) \sin(\phi(t) + \phi_L^{ch}(t)) + E^{ch}(t) \quad (4)$$

$$AR^{ch}(t)|_{t=\psi^{-1}(\omega)} = AR(\omega) \quad (5)$$

$$\phi_L^{ch}(t)|_{t=\psi^{-1}(\omega)} = \phi_L(\omega) \quad (6)$$

$$E^{ch}(t) \underset{t \rightarrow \infty}{=} 0 \quad (7)$$

<sup>83</sup> Angular frequency,  $\omega = \psi(t) = \frac{d\phi(t)}{dt}$ , is a known quantity from the one-to-one mapping between time and frequency of the input chirp signal.

Table 1: Example systems

Sl.no	System	Remarks
1	$\frac{2}{0.01s+1}$	First-order system
2	$\frac{2}{(0.01s)^2+0.02s+1}$	Second-order critically damped system
3	$\frac{2(s+20)}{(s+100)(s+30)}$	Second-order overdamped system with a zero in left half plane
4	$\frac{40}{(s+200)^2}$	System with real repeated poles
5	$\frac{2}{(s+400)^2(s^2+200s+10000)}$	$4^{th}$ -order system with real repeated poles and complex conjugate poles
6	$\frac{20}{(s+100+400i)^2(s+100-400i)^2}$	$4^{th}$ -order system with repeated complex-conjugate pairs as poles

In summary, the asymptotic output response of the system to an input chirp signal can be written as:

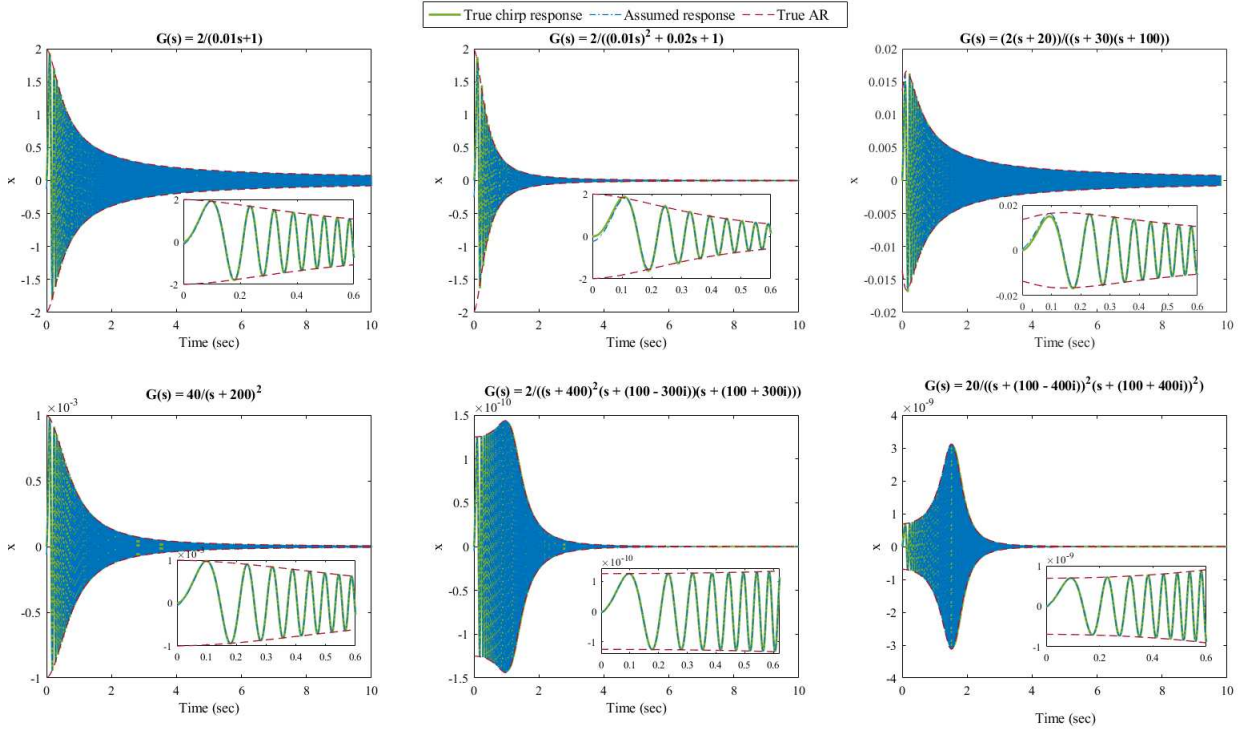
$$x(t) = A_{in} AR(\psi(t)) \sin(\phi(t) + \phi_L(\psi(t))) \quad (8)$$

We will now validate the claims proposed in this paper through simulation studies. While we have validated the claims on a large number of linear systems with different characteristics, we report results for six different systems of various characteristics in terms of zeros, poles (repeated and not repeated), and orders as shown in Table 1. To validate the claim, we compare the true chirp response ( $x(t)$ ) of these systems to unit amplitude chirp input and the asymptotic output behavior  $x(t)$  as predicted by (8) in Figure 2. Responses corresponding to both linear and fourth order chirp inputs are provided. Linear chirp input signal that is used sweeps frequencies from 1 Hz to 400 Hz in 10 seconds, while the fourth order chirp input used for the study sweeps frequencies from 1 Hz to 1000 Hz in 10 seconds. An immediate observation from Figure 2 is that in both cases, the envelope of  $x(t)$  converges to the true  $AR$  and  $x(t)$  converges to  $x(t)$ , very rapidly, within a couple of cycles. To illustrate this, the error  $(x(t) - x(t))$  is plotted in Figure 3 for both linear and fourth order chirp responses. It can be seen that the error converges to zero within a short time for both linear and fourth order chirp signals.

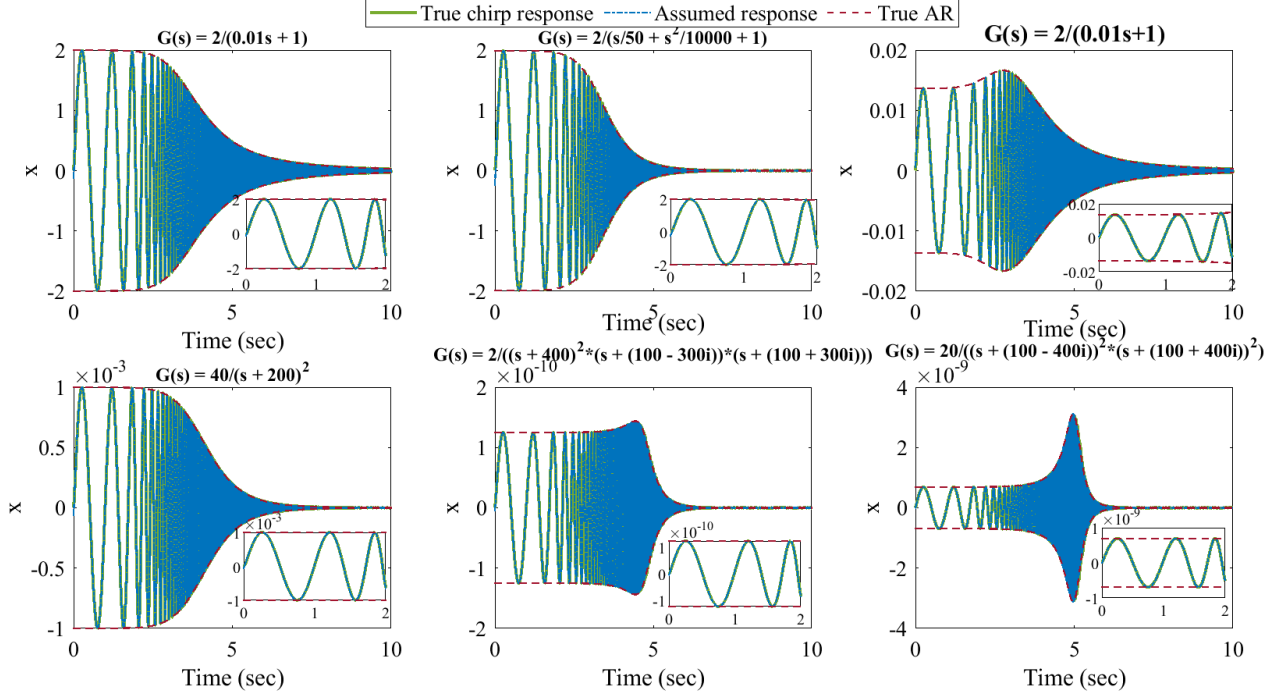
The choice of the phase function does have an effect on the speed at which the errors might vanish. However, remarkably, the one-to-one time frequency relationship is retained for different phase functions. The theoretical analysis and the proofs presented in [27] describe the mathematics that underlie these observations. The Nyquist plots generated for these examples are provided in Figure 4. It can be seen that the Nyquist profiles match the theoretically computed ones extremely accurately. The chirp signal-based FRA using more than 50000 samples takes approximately 0.25 seconds in an eighth generation i7 processor and thus, is not computationally expensive. It can also be seen that response for a larger frequency range is obtained using a fourth order chirp compared to a linear chirp signal in the same duration. However, for the same experimentation time, within the range of frequency covered by the linear chirp, the resolution will be better for the linear chirp than the fourth order chirp. These simulation results demonstrate the significant application potential for chirp-based FRA.

### 3 Discussion

The first thing to notice about the *main result* is that this is also an asymptotic result (much like *Lemma 1*), where a certain time profile for the output remains after the transients vanish. However, the final time profile that is shown to be retained is the key difference between *Lemma 1* and the *main result*. In *Lemma 1*, the time profile is a sinusoid of a fixed frequency and a constant amplitude and phase lag. However, in the *main result*, the time profile is a chirp signal with time varying frequency, amplitude and phase. Let us remember that the differential of the phase of the sinusoid (time function) was defined as the instantaneous frequency at a time point. The amplitude and phase of the output are time functions. Since we have an one-to-one equivalence between time and frequency, we can replace the time variable in the expressions for magnitude and phase with the corresponding frequency function. This would result in magnitude and phase becoming functions of frequency.



(a) Linear Chirp Response



(b) Fourth order Chirp Response

Figure 2: Response of various systems to linear and fourth order chirp inputs. Zoomed responses are given in the inset.

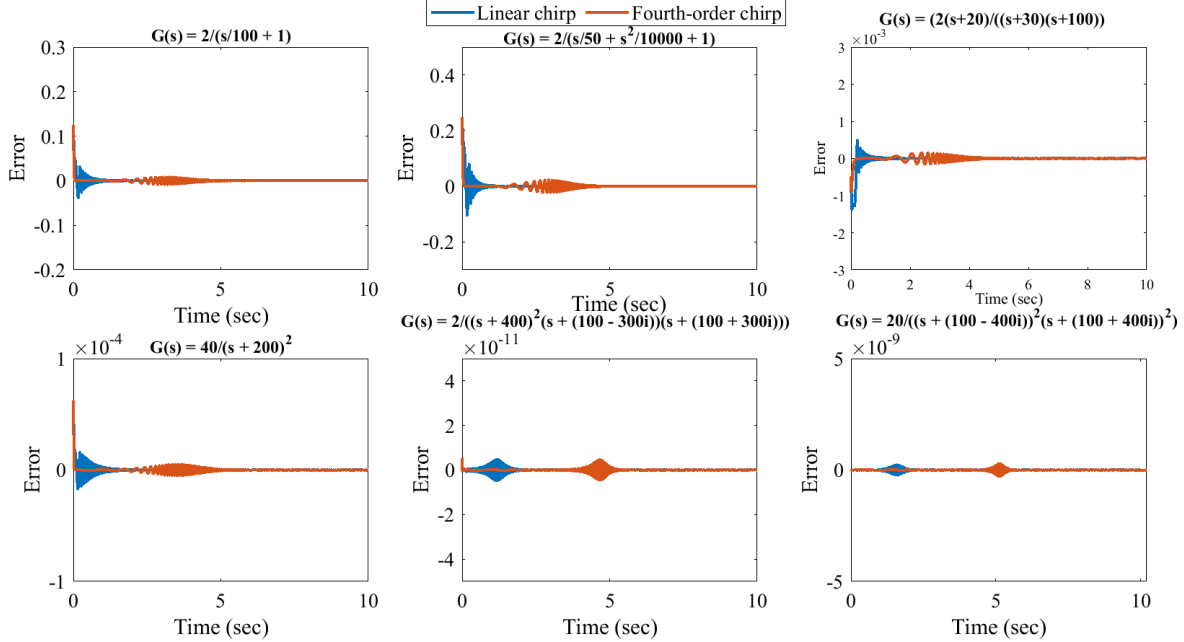


Figure 3: Error between actual chirp response ( $x(t)$ ) and assumed chirp response  $A_{in}AR(\psi(t))\sin(\phi(t) + \phi_L(\psi(t)))$  for linear and fourth order chirp responses

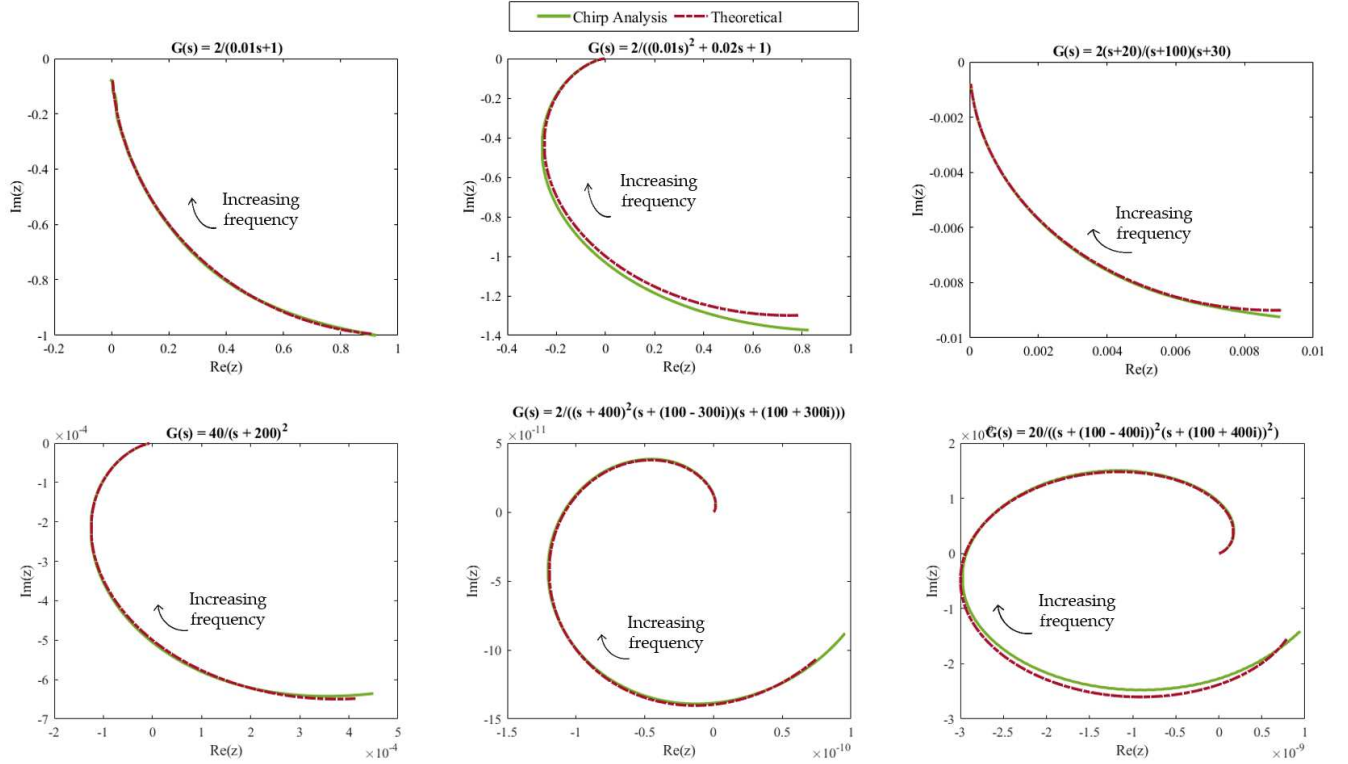
119     The main result now provides a remarkable equivalence in that the frequency functions so derived from  
 120     the output time profiles are exactly equal to the corresponding frequency response functions that would have  
 121     resulted from applying Lemma 1 for multiple frequencies, once transients vanish. In other words, we now  
 122     have one frequency defined for every time point and incredibly, all the frequency information is located at  
 123     that time point. Of course, it is important to reiterate that this is an asymptotic property (like Lemma  
 124     1); however, we have demonstrated that the error vanishes very rapidly, making this result of tremendous  
 125     practical value much like the result described in Lemma 1, which has been used for decades now.

126     The most important implication of this result is that the time required for identifying the FR of the  
 127     system can be brought down dramatically. This is illustrated in Figure 1, where one sees that a single point  
 128     in the Nyquist plot corresponds to a signal in FR analysis. In the series of sines approach, these signals are  
 129     combined serially and this increases the testing times significantly. In the sum of the sines approach, these  
 130     signals are overlaid; however, to generate a point in the Nyquist plot, the output has to be deconvolved as  
 131     responses to each of these sine signals and issues related to spectral leakage and other difficulties need to  
 132     be addressed [29, 7]. Further, the length of the signal is determined by the lowest frequency that one is  
 133     interested in exploring. The main result in this paper provides us a totally new approach to solving this  
 134     problem, wherein a single time point in the input signal corresponds to one point in the Nyquist plot (Figure  
 135     1). This allows the exploration of multiple frequencies in dramatically reduced experimentation time.

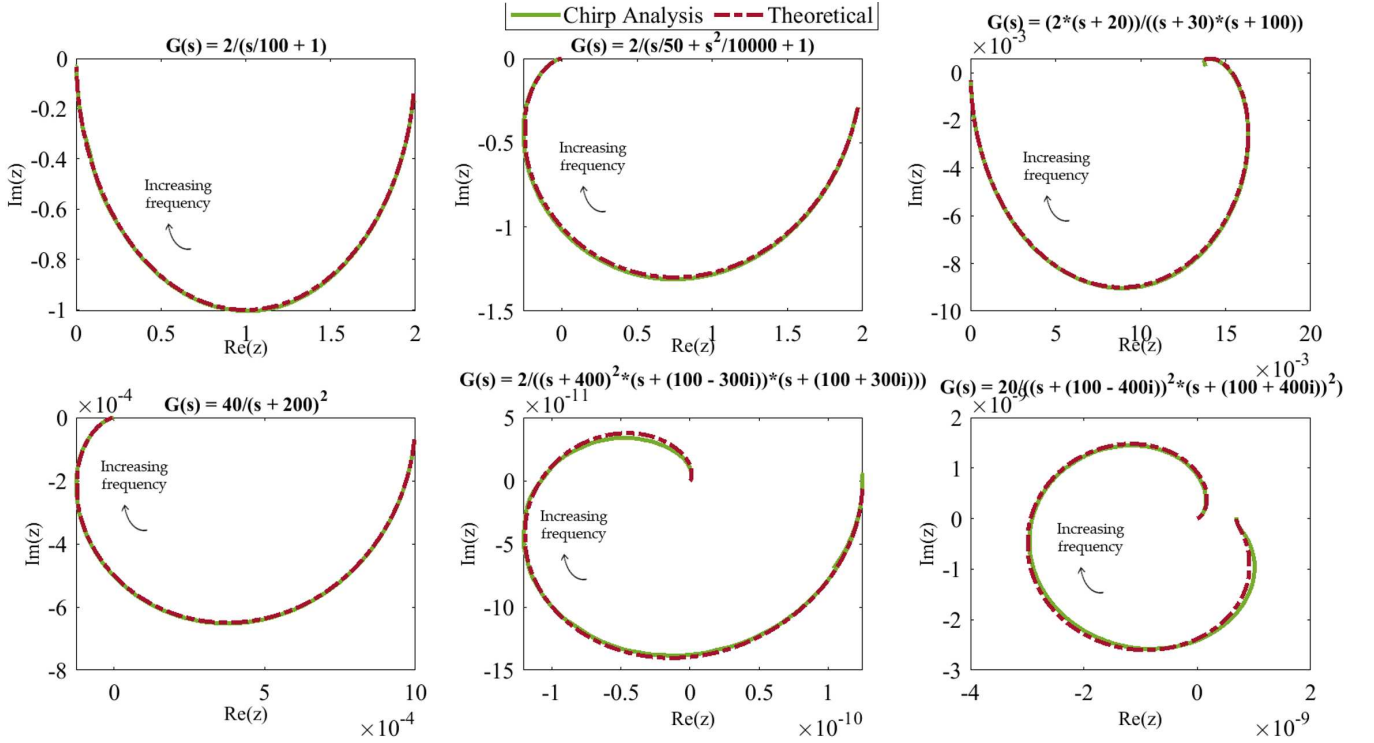
136     We have presented the key statement of the main result here. All the theoretical underpinnings and a  
 137     proof for this result for general linear systems with repeated and non-repeated poles along with conditions on  
 138     admissible phase functions are all comprehensively described in [27]. One can see that many functional forms  
 139     can satisfy the conditions for admissible phase function; however, from a practical demonstration viewpoint  
 140     we will focus on polynomial chirp signals in this paper.

### 141     3.1 Relevance to Electrochemical Impedance Spectroscopy

142     While FRA is used in almost all engineering fields, in this section, we will show the relevance of the theo-  
 143     retical developments reported in this paper for electrochemical impedance spectroscopy (EIS). The notion  
 144     of impedance has been around since the late 1800s with impedance being defined for the first time by Oliver  
 145     Heaviside and this quantity represented as a complex number by Arthur Kennelly in the 1890s [19]. EIS



(a) Nyquist plots generated using linear chirp response



(b) Nyquist plots generated using fourth order chirp response

Figure 4: Nyquist plots generated using linear and fourth order chirp analysis in comparison with the theoretical frequency response for various systems. Nyquist plots generated using linear and fourth order chirp responses are for the input frequency range [1Hz 400Hz] and [1Hz 1000Hz] respectively.

Table 2: Comparison of standard EIS and chirp signal-based EIS

(a) General comparison

	Standard EIS	Chirp signal-based EIS
Input signal	Sinusoidal	Chirp (Linear/Polynomial)
Frequency of input signal	Constant	Varying
No. of signals needed	Depends on the no. of frequencies needed	1
Time required	Depends on the no. of frequencies needed	Depends on the frequency range
No. of data points in the plot	Same as no. of signals	Same as total samples in the signal

(b) Example with fourth order chirp input that sweeps through the frequency range 0.001Hz to 10000Hz at a sampling rate,  $r = 10,000$  samples/sec

	Standard EIS	Chirp signal-based EIS
Input signal	$A_{in} \sin(2\pi ft)$	$A_{in} \sin(\phi(t)); \quad \phi = P_5(t); \quad f = \frac{d\phi}{dt}$
Output signal (steady-state)	$A_{in} AR \sin(2\pi ft + \phi_L)$	$A_{in} AR^{ch}(t) \sin(\phi(t) + \phi_L^{ch}(t))$
No. of signals needed	60 (Assume)	1
No. of cycles per signal needed	2 (Assume)	-
Signal duration, $T$	2.66 hours	100 sec
No. of data points in the plot	60	$10^6 (= r \times T)$

is essentially FRA of systems with the input and output being current and voltage respectively. EIS has been used for diagnostics in various electrochemical systems finding applications in disparate problem domains such as corrosion studies [22, 23], sensors [18], biological systems [9, 14], concrete characterization [2, 24], body fat estimation [12], and many others. Impedance as a diagnostic measure cross-cuts almost all engineering and science disciplines. In view of this universality and continued relevance, there have been thousands of papers that have been devoted to this field. For example, Google scholar has 44603 articles with the keyword ‘Electrochemical Impedance Spectroscopy’ just for a two year period from 2018. Similarly, ScienDirect and Scopus has 38,727 and 59,856 articles with the same keyword for the same duration.

We are now in a position to describe the impact of the *main result* reported in this paper on EIS. If the chirp analysis procedure is followed instead of a series of sinusoidal signals for EIS, then the significance will become apparent. Table 2b outlines the advantages of chirp signals for EIS assuming a frequency range 1 mHz to 10 kHz with a sampling rate of 10000 samples/sec and a fourth order chirp signal. It can be seen that chirp analysis will require only 100 seconds to extract impedance information for  $10^6$  different frequencies, while standard EIS analysis would require 2.66 hours to extract the impedance information for 60 different frequencies. Table 2a summarizes the main features of the chirp signal-based EIS.

## 4 Methods

Based on the *main result*, it is possible to extract the entire frequency response using a single chirp perturbation experiment unlike standard FRA, where ‘ $n$ ’ sinusoidal perturbation experiments would be required to acquire frequency information for ‘ $n$ ’ different frequencies with a series of sines. As discussed already, if a multi-sine signal were to be used, the time required would still be dictated by the smallest frequency of interest. As a corollary to the *main result*, a procedure for generating the Nyquist plot (polar representation of the frequency response obtained by expressing amplitude ratio and phase lag as a complex number) can be developed as shown below:

1. Perturb the system with a chirp input signal of amplitude  $A_{in}$  and collect the system’s response
2. Obtain the outer envelope of output signal to obtain  $A^{ch}$
3. Calculate amplitude ratio,  $AR^{ch} = \frac{A^{ch}}{A_{in}}$
4. Calculate output phase ( $\phi + \phi_L^{ch}$ ) using (8)

- 173 5. Unwrap the output phase to a smooth monotonically increasing function
- 174 6. Calculate phase lag,  $\phi_L^{ch}$ , by subtracting the input phase ( $\phi$ ) from the output phase obtained in Step 4
- 175 7. Generate Nyquist plot using the complex number,  $z(\omega) = AR^{ch}(\omega)e^{i\phi_L^{ch}(\omega)}$

176 **5 Conclusions**

177 In summary, a novel result of this work is that it is possible to extract the entire frequency response from  
 178 short-term time signals. This result is supported through theoretical analysis and extensive simulation  
 179 results. The analysis provides an initial assessment of the rate of convergence of the error term. We have  
 180 verified this result for a large number of linear systems with different characteristics (in terms of zeros and  
 181 poles). Theoretical proof of its validity for any general linear system is provided elsewhere ([27]). The  
 182 relationship between error convergence rates and the choice of phase functions should be more carefully  
 183 explored. Further, the implications of this approach *vis a vis* the notion of harmonics in frequency response  
 184 analysis of nonlinear systems need to be explored. Additionally, we have considered monotonically increasing  
 185 frequency functions, similar analysis needs to be performed for non-monotonic functions. This can open up  
 186 new ideas for simple nonlinearity detection techniques purely from the response to an appropriately designed  
 187 chirp signal. Further, the implications of this result from a general system identification viewpoint needs  
 188 to be assessed. While it has been shown, conceptually, that the whole frequency response can be extracted  
 189 with large bandwidth short-time signals, there are several practical implementation issues that need to be  
 190 addressed. These are concerns related to the effect of noise, sampling rates, and non-stationarities. Some  
 191 of our initial work has started to address these practical implementation issues [6, 28]. More sophisticated  
 192 iterative algorithms for processing the chirp response data can be developed that can minimize, even more,  
 193 the effect of error terms in the initial segment of data and the corresponding frequency response identification.

194 Other than the literature associated with system identification, the approach described in this paper  
 195 has a role to play in all fields where impedance is used. Impedance being a fundamental characteristic of  
 196 the system, has been used in various applications [24, 23, 14]; however, many of these studies were limited  
 197 to higher frequencies ( $> 1\text{Hz}$ ) as the time required for impedance generation at low frequencies is usually  
 198 unacceptably large. Since the impedance information from chirp analysis is obtained in a much shorter time  
 199 (even at low frequencies), chirp analysis has the potential to become the technique of choice for EIS in all of  
 200 these applications.

201 **References**

- 202 [1] Jonathan Allen. Short term spectral analysis, synthesis, and modification by discrete fourier transform.  
*IEEE Transactions on Acoustics, Speech, and Signal Processing*, 25(3):235–238, 1977.
- 203 [2] Venu Gopal Madhav Annamdas, Yaowen Yang, and Chee Kiong Soh. Impedance based concrete monitoring using embedded pzt sensors. *International Journal of Civil & Structural Engineering*, 1(3):414–424, 2010.
- 204 [3] Fabusuyi A Aroge and Paul S Barendse. Time-frequency analysis of the chirp response for rapid  
 205 electrochemical impedance estimation. In *2018 IEEE Energy Conversion Congress and Exposition (ECCE)*, pages 2047–2052. IEEE, 2018.
- 206 [4] Boualem Boashash. Estimating and interpreting the instantaneous frequency of a signal. I. Fundamentals. *Proceedings of the IEEE*, 80(4):520–538, 1992.
- 207 [5] Pierre Borgnat and Patrick Flandrin. On the chirp decomposition of weierstrass–mandelbrot functions,  
 208 and their time–frequency interpretation. *Applied and Computational Harmonic Analysis*, 15(2):134–146,  
 209 2003.
- 210 [6] Brian Bullecks, Resmi Suresh, and Raghunathan Rengaswamy. Rapid impedance measurement using  
 211 chirp signals for electrochemical system analysis. *Computers & Chemical Engineering*, 106:421–436,  
 212 2017.

- 218 [7] Byoung-Yong Chang and Su-Moon Park. Electrochemical impedance spectroscopy. *Annual Review of*  
219 *Analytical Chemistry*, 3:207–229, 2010.
- 220 [8] Eric Chassande-Mottin and Patrick Flandrin. On the time-frequency detection of chirps. *Applied and*  
221 *Computational Harmonic Analysis*, 6(2):252–281, 1999.
- 222 [9] CHRIS Clausen, SIMON A Lewis, and JARED M Diamond. Impedance analysis of a tight epithelium  
223 using a distributed resistance model. *Biophysical journal*, 26(2):291–317, 1979.
- 224 [10] Kazimierz Darowicki and Paweł Ślepski. Determination of electrode impedance by means of exponential  
225 chirp signal. *Electrochemistry communications*, 6(9):898–902, 2004.
- 226 [11] Ingrid Daubechies. The wavelet transform, time-frequency localization and signal analysis. *IEEE*  
227 *transactions on information theory*, 36(5):961–1005, 1990.
- 228 [12] P Deurenberg, Angela Andreoli, P Borg, K Kukkonen-Harjula, A De Lorenzo, Wouter D Van  
229 Marken Lichtenbelt, Giulio Testolin, R Vigano, and Niels Vollaard. The validity of predicted body  
230 fat percentage from body mass index and from impedance in samples of five european populations.  
231 *European journal of clinical nutrition*, 55(11):973–979, 2001.
- 232 [13] Patrick Flandrin. Time frequency and chirps. In *Wavelet Applications VIII*, volume 4391, pages 161–175.  
233 International Society for Optics and Photonics, 2001.
- 234 [14] Samira Ghasemi, Mariam T Darestani, Zohreh Abdollahi, and Vincent G Gomes. Online monitoring of  
235 emulsion polymerization using electrical impedance spectroscopy. *Polymer International*, 64(1):66–75,  
236 2015.
- 237 [15] Nabil Hentati, Hanno Reckmann, and Ingolf Wassermann. Identification of the channel frequency  
238 response using chirps and stepped frequencies, November 18 2008. US Patent 7,453,372.
- 239 [16] Norden E Huang, Zheng Shen, Steven R Long, Manli C Wu, Hsing H Shih, Quanan Zheng, Nai-Chyuan  
240 Yen, Chi Chao Tung, and Henry H Liu. The empirical mode decomposition and the hilbert spectrum  
241 for nonlinear and non-stationary time series analysis. *Proceedings of the Royal Society of London. Series*  
242 *A: mathematical, physical and engineering sciences*, 454(1971):903–995, 1998.
- 243 [17] Masayuki Itagaki, Yusuke Gamano, Yoshinao Hoshi, and Isao Shitanda. Determination of electrochemical  
244 impedance of lithium ion battery from time series data by wavelet transformation-uncertainty of  
245 resolutions in time and frequency domains. *Electrochimica Acta*, 332:135462, 2020.
- 246 [18] Audrey M Johnson, Donald R Sadoway, Michael J Cima, and Robert Langer. Design and testing of an  
247 impedance-based sensor for monitoring drug delivery. *Journal of the Electrochemical Society*, 152(1):H6,  
248 2004.
- 249 [19] Arthur E. Kennelly. Impedance. *Transactions of the American Institute of Electrical Engineers*, X:175–  
250 216, 1893.
- 251 [20] Uday Khankhoje and VM Gadre. Optimal fractional fourier domains for quadratic chirps. *IETE journal*  
252 *of research*, 52(1):65–70, 2006.
- 253 [21] Patrick J Loughlin and Berkant Tacer. Comments on the interpretation of instantaneous frequency.  
254 *IEEE Signal Processing Letters*, 4(5):123–125, 1997.
- 255 [22] DV Ribeiro and JCC Abrantes. Application of electrochemical impedance spectroscopy (EIS) to monitor  
256 the corrosion of reinforced concrete: a new approach. *Construction and Building Materials*, 111:98–104,  
257 2016.
- 258 [23] PR Roberge and VS Sastri. On-line corrosion monitoring with electrochemical impedance spectroscopy.  
259 *Corrosion*, 50(10):744–754, 1994.

- 260 [24] Sanita Rubene, Martins Vilnitis, and Juris Noviks. Frequency analysis for EIS measurements in auto-  
261 claved aerated concrete constructions. *Procedia Engineering*, 108:647–654, 2015.
- 262 [25] B Sanchez, G Vandersteen, R Bragos, and J Schoukens. Optimal multisine excitation design for broad-  
263 band electrical impedance spectroscopy. *Measurement Science and Technology*, 22(11):115601, 2011.
- 264 [26] P Slepški and Kazimierz Darowicki. Optimization of impedance measurements using ‘chirp’ type per-  
265 turbation signal. *Measurement*, 42(8):1220–1225, 2009.
- 266 [27] Resmi Suresh and Raghunathan Rengaswamy. Proof for frequency response analysis using chirp signals.  
267 *arXiv e-prints*, pages arXiv–2008, 2020.
- 268 [28] Resmi Suresh, Sathish Swaminathan, and Raghunathan Rengaswamy. Rapid impedance spectroscopy  
269 using dual phase shifted chirp signals for electrochemical applications. *International Journal of Hydrogen  
270 Energy*, 45(17):10536–10548, 2020.
- 271 [29] Edwin Van der Ouderaa, Johan Schoukens, and Jean Renneboog. Peak factor minimization using a  
272 time-frequency domain swapping algorithm. *IEEE Transactions on Instrumentation and Measurement*,  
273 37(1):145–147, 1988.
- 274 [30] Jacob Verhulst, Mohamed Belkhayat, SHEN Zhiyu, Marko Jaksic, Paolo Mattavelli, and Dushan Boroyevich.  
275 System and method for impedance measurement using chirp signal injection, April 11 2017. US  
276 Patent 9,618,555.

# Figures

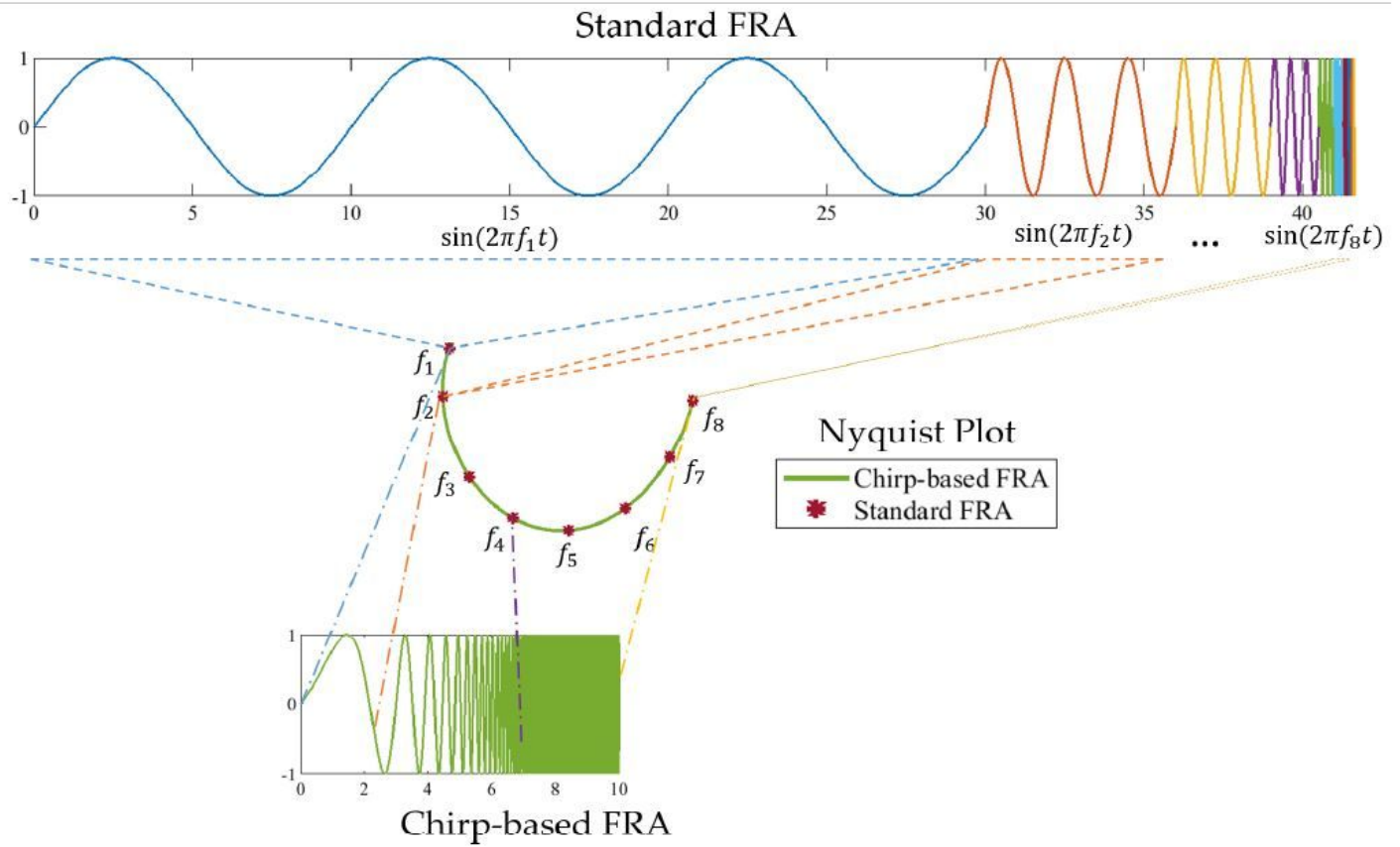
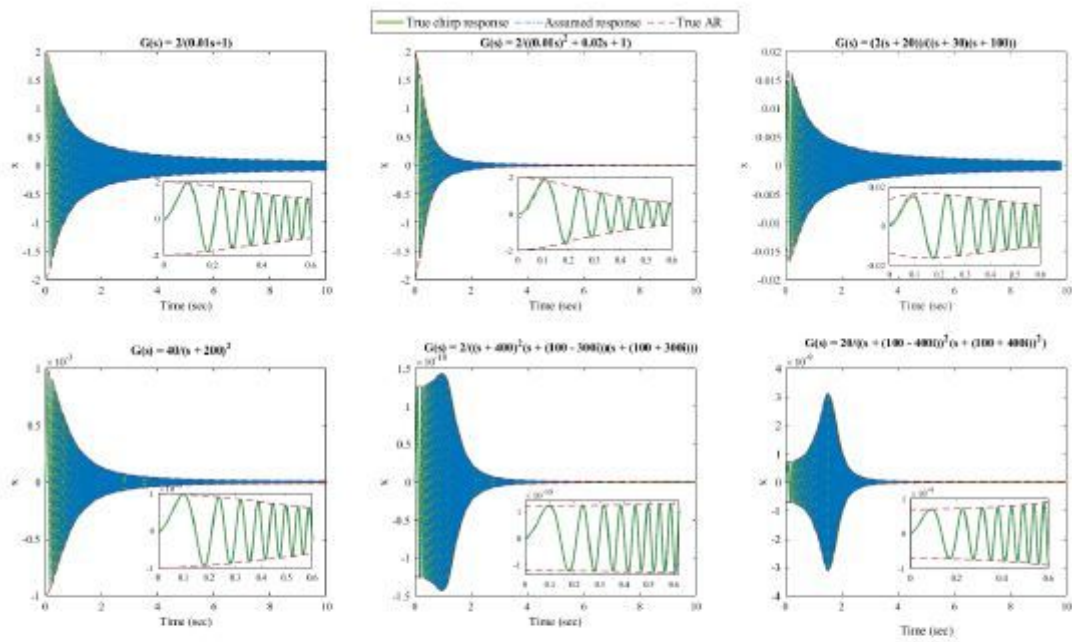
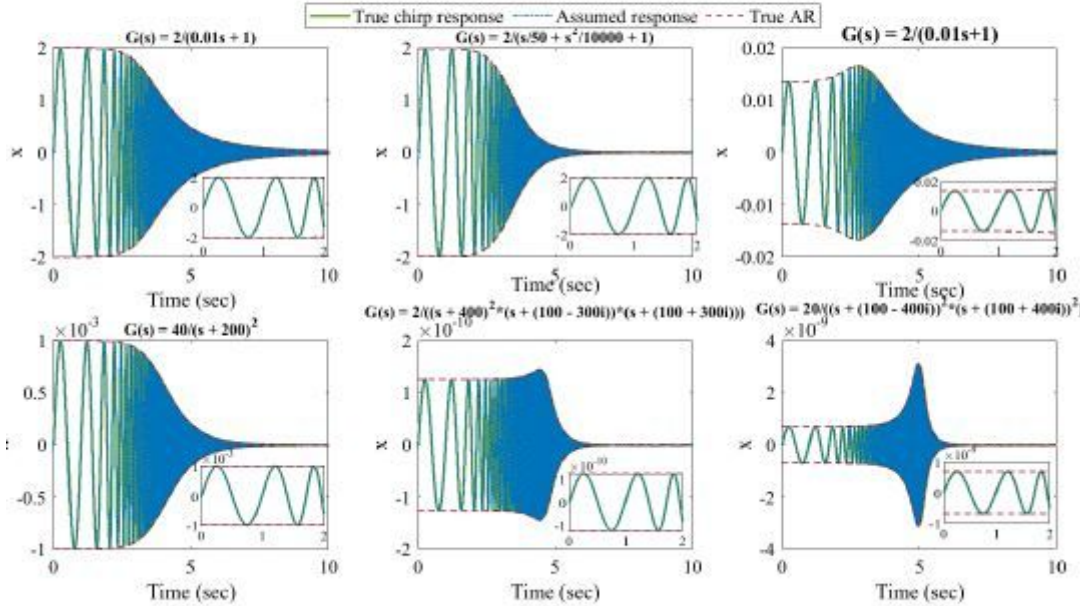


Figure 1

Comparison of the working of standard FRA and chirp-based FRA. Standard FRA uses a few cycles of multiple sinusoidal signals of different frequencies to obtain discrete points in the Nyquist plot. Chirp-based FRA generates as many points in Nyquist plot as the number of samples in the output signal and thus, a smooth and continuous impedance profile is obtained in a short time.



(a) Linear Chirp Response



(b) Fourth order Chirp Response

## Figure 2

Response of various systems to linear and fourth order chirp inputs. Zoomed responses are given in the inset.

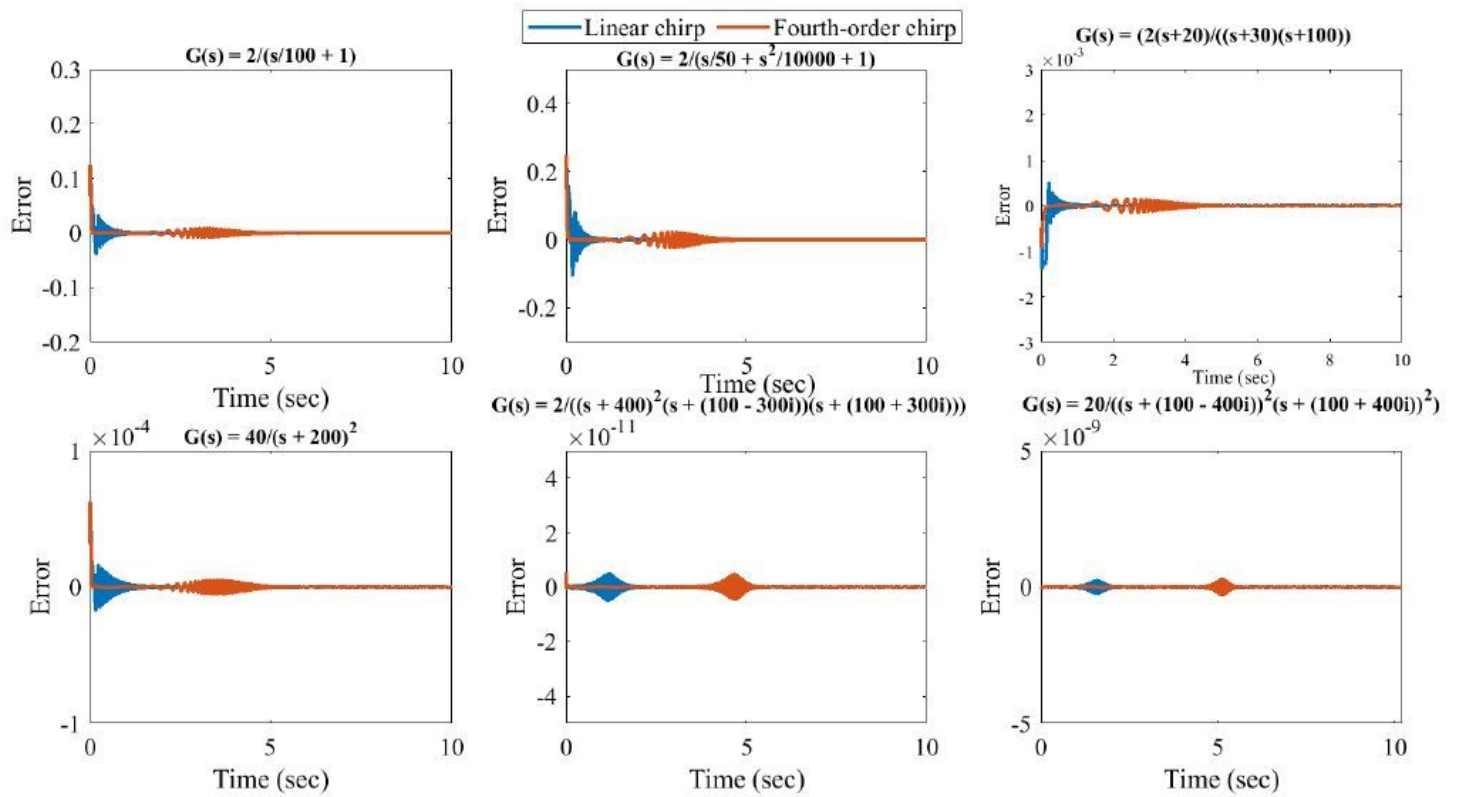
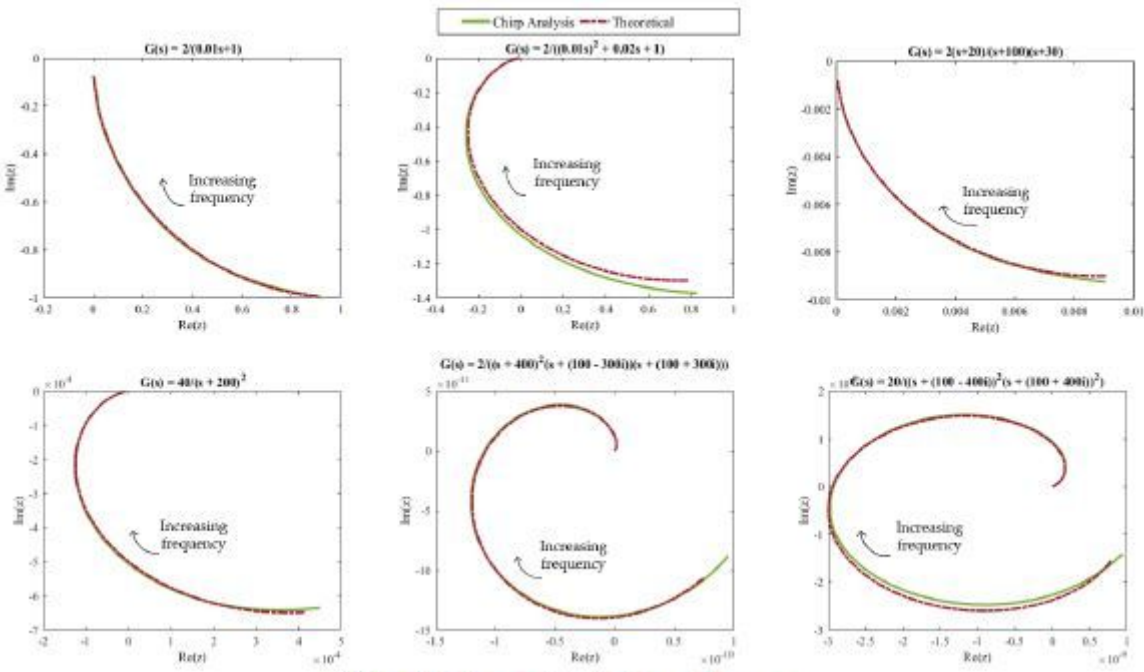
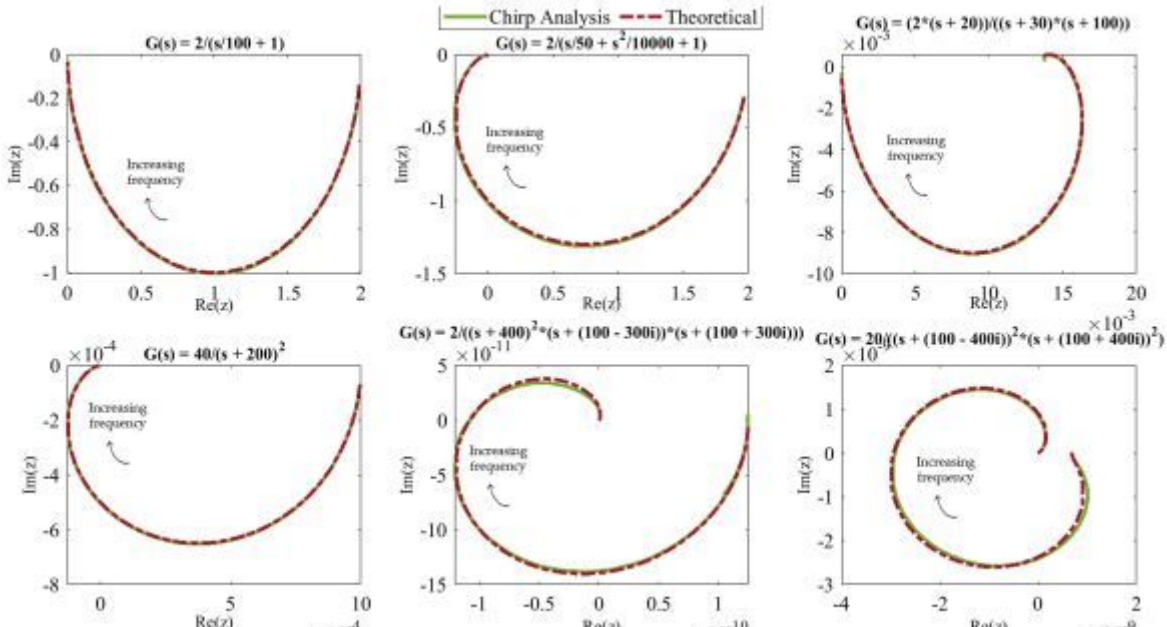


**Figure 3**

Error between actual chirp response ( $x(t)$ ) and assumed chirp response  $AinAR( (t)) \sin(\omega(t) + \phi L( (t)))$  for linear and fourth order chirp responses



(a) Nyquist plots generated using linear chirp response



(b) Nyquist plots generated using fourth order chirp response

**Figure 4**

Nyquist plots generated using linear and fourth order chirp analysis in comparison with the theoretical frequency response for various systems. Nyquist plots generated using linear and fourth order chirp responses are for the input frequency range [1Hz 400Hz] and [1Hz 1000Hz] respectively.